

A peer-reviewed version of this preprint was published in PeerJ on 28 April 2015.

[View the peer-reviewed version](https://doi.org/10.7717/peerj.904) (peerj.com/articles/904), which is the preferred citable publication unless you specifically need to cite this preprint.

Kato Y. 2015. Tunable translational control using site-specific unnatural amino acid incorporation in *Escherichia coli*. PeerJ 3:e904
<https://doi.org/10.7717/peerj.904>

Tunable translational control using site-specific unnatural amino acid incorporation in *Escherichia coli*

Yusuke Kato

Translation of target gene transcripts in *Escherichia coli* harboring UAG amber stop codons can be switched on by the amber-codon-specific incorporation of an exogenously supplied unnatural amino acid, 3-iodo-L-tyrosine. Here, we report that this translational switch can control the translational efficiency at any intermediate magnitude by adjustment of the 3-iodo-L-tyrosine concentration in the medium, as a tunable translational controller. The translational efficiency of a target gene reached maximum levels with 10^{-5} M 3-iodo-L-tyrosine, and intermediate levels were observed with suboptimal concentrations (approximately spanning a 2-log_{10} concentration range, 10^{-7} to 10^{-5} M). Such intermediate-level expression was also confirmed in individual bacteria.

2 Author(s):

3 Yusuke Kato

4

5 Affiliation & Location:

6 Genetically Modified Organism Research Center,

7 National Institute of Agrobiological Sciences,

8 Tsukuba, Ibaraki, Japan.

9

10 *Address for correspondence:

11 Yusuke Kato, Ph.D.

12 Genetically Modified Organism Research Center

13 National Institute of Agrobiological Sciences

14 Oowashi 1-2

15 Tsukuba, Ibaraki, Japan

16 Phone/Fax: +81-29-838-6059

17 Email: kato@affrc.go.jp

18 **Abstract**

19

20 Translation of target gene transcripts in *Escherichia coli* harboring UAG amber stop codons can be

21 switched on by the amber-codon-specific incorporation of an exogenously supplied unnatural amino

22 acid, 3-iodo-L-tyrosine. Here, we report that this translational switch can control the translational

23 efficiency at any intermediate magnitude by adjustment of the 3-iodo-L-tyrosine concentration in the

24 medium, as a tunable translational controller. The translational efficiency of a target gene reached

25 maximum levels with 10^{-5} M 3-iodo-L-tyrosine, and intermediate levels were observed with suboptimal

26 concentrations (approximately spanning a 2-log_{10} concentration range, 10^{-7} to 10^{-5} M). Such

27 intermediate-level expression was also confirmed in individual bacteria.

28

29 **Introduction**

30

31 Controlling gene expression is a key methodology for biotechnology. Particularly, its fine-tuning and
32 optimization are important for construction of artificial gene circuits in synthetic biology and for
33 metabolic engineering. Tunable conditional expression systems regulated by extracellular
34 inducers/repressors are thus very useful.

35 We previously demonstrated a translational switch using site-specific unnatural amino acid
36 (UAA) 3-iodo-L-tyrosine (IY) incorporation in natural amber suppressor-free strains of *Escherichia*
37 *coli* (Minaba and Kato, 2014). The translational switch is based on conditional read-through of the
38 UAG amber stop codons that are inserted in target genes (Fig. 1). A variant of aminoacyl-tRNA
39 synthetase (aaRS) IYRS that was derived from the archaeobacterium *Methanocaldococcus jannaschii*
40 specifically recognizes both IY and an amber suppressor tRNA (tRNA_{CUA}) MJR1 (Sakamoto et al.,
41 2009). Extracellular IY is taken up and incorporated into proteins at sites of the amber codons in the
42 IYRS/ MJR1-expressing cells. The target gene transcripts with the amber stop codons inserted next to
43 the AUG translational start codon are translated only in the presence of IY. The absence of IY prevents
44 translation of the target genes.

45 The UAA-controlling translational switch has distinct features for gene regulation (Minaba
46 and Kato, 2014). First, this translational switch also can be controlled by the induction/repression of

47 either aaRS or tRNA_{CUA}, in addition to the presence/absence of UAA. The switchability can be
48 modulated by combination use with aaRS- and/or tRNA_{CUA}- switching. Second, UAA does not
49 naturally exist. In addition, UAA is a “building block” that forms an aminoacyl-tRNA and target
50 proteins, distinct from simple regulation-specific molecules, such as isopropyl β-D-1-
51 thiogalactopyranoside (IPTG) for the derepression of the lactose operator. The switching mechanism
52 involves the direct incorporation of UAA into target proteins, and is not effective for interventional
53 systems. Thus, the UAA-controlling translational switch is robust against environmental and host-
54 endogenous noises. Although an inducible tRNA_{CUA} has been used as a similar translational switch
55 based on amber suppression, these features are not found (Zengel and Lindahl, 1981; Herring et al.,
56 2003). Third, the UAA-controlling translational switch can be used in combination with any
57 established transcriptional switches to obtain a synergistic regulatory effect. Using this strategy, we
58 constructed a high-yield and zero-leakage expression system, in which strong expression by the T7
59 promoter was maintained under the induction condition, and almost no proteins were expressed under
60 the repression condition by double control of transcription-translation. Riboswitches and small
61 regulatory RNAs (sRNAs) are well known as post-transcriptional controlling tools in *E. coli*. Some
62 riboswitches that are located in non-coding portions of mRNAs can regulate gene expression *in cis* by
63 binding a specific small molecule via controlling translational initiation and/or mRNA degradation
64 (Caron et al., 2012). The sRNAs are trans-acting and target gene alterations are not required, although

65 off-target effects are often detected (Bobrovskyy and Vanderpool, 2013). The sRNAs modulate the
66 translation via controlling translation initiation and/or mRNA degradation. The distinct characteristics
67 of these RNA-based post-transcriptional switches suggest that the UAA-controlling translational
68 switch is complementary rather than competitive with the others. To date, many systems for the
69 incorporation of various UAAs have been developed (Liu and Schultz, 2010). In addition, similar
70 translational switches controlled by UAAs are expected to be applicable also for eukaryotes, such as
71 yeasts, nematodes, insects, mammalian cells, and plants, because the site-specific unnatural amino acid
72 incorporation systems have already been introduced (Chin et al., 2003; Greiss and Chin, 2011; Bianco
73 et al., 2012; Sakamoto et al., 2002; Li et al., 2013). The target gene products that are controlled by the
74 UAA-controlling translational switch necessitate the incorporation of UAA. Although this is primarily
75 a disadvantage because of probable functional alterations in some target proteins, we can avoid this
76 problem by neutral site selection, incorporation into tag or processed-out sequences. Alternatively, the
77 UAAs can be used as tools to facilitate purification or tracking of target gene products (Minaba and
78 Kato, 2014).

79 In previous studies, we only focused on the on-off aspect of the IY-controlling translational
80 switch. Here, we studied the intermediate states between the fully on- and off-states of the translational
81 switch. The results suggest that this switch can control the translational efficiency at any intermediate
82 magnitude by adjustment of the appropriate IY concentration, and thus, function as a tunable

83 translational controller.

84

85 **Materials and Methods**

86

87 *Fluorescence measurement of pooled bacteria*

88 Assays were performed as described previously (Minaba and Kato, 2014). Briefly, we used *E. coli*

89 BL21-AI [*F⁻ ompT gal dcm lon hsdS_B(r_B⁻ m_B⁻) araB::T7RNAP-tetA*] carrying the plasmid pTYR

90 MjIYRS2-1(D286) MJR1×3 encoding IYRS and MJR1 and the amber-inserted EGFP expression

91 plasmid (driven by the *E. coli lpp* promoter with an amber stop codon TAG inserted next to the start

92 codon ATG). The sequence for the EGFP expression plasmid is shown in Fig. S1. An overnight

93 (approximately 16 h) culture of bacteria was resuspended in an equal volume of liquid LB medium

94 (1% bacto tryptone, 0.5% yeast extract, and 1% NaCl) containing various concentrations of optically-

95 pure IY. IY was directly dissolved and diluted in LB medium. After a 6 h culture (2 ml in a 14 ml-

96 culture tube at 37°C with rotary shaking at 200 rpm), the bacteria were collected by centrifugation

97 (1,800 × g for 3 min). The pellet was washed and was resuspended in an equal volume of 0.9% (wt/vol)

98 NaCl, and this wash step was repeated twice. An aliquot of the bacterial suspension (150 μl) was

99 diluted in 3.0 ml of the 0.9% NaCl, and the OD₅₉₀ was measured. The fluorescence intensity of the

100 bacterial population was measured using a Shimadzu RF-5300PC spectrofluorometer (excitation, 480

101 nm; emission, 515 nm). The background fluorescence was estimated using the bacteria carrying a

102 MJR1-deleted plasmid (ΔMJR1) at IY=0 (no significant IY-dependency was observed, Fig. S2). The

103 background-subtracted values are used to calculate the points for the dose-response curve. For the time
104 course measurement of EGFP accumulation, we cultured the bacteria in 20 ml LB medium in a 200 ml
105 culture flask. Aliquots of the bacterial culture (150 μ l) were withdrawn at various time points, and the
106 OD₅₉₀ and fluorescence were measured.

107
108 *Photomicrographs*

109 Photomicrographs and Nomarski differential interference contrast images of the fluorescent bacteria
110 were recorded using both a Carl Zeiss Axioskop 2 with a 38-HE Endow GFP filter-set and a Roper
111 Scientific Photometrics CoolSNAP ver.1.1.

112
113 *Image analyses*

114 Analyses of the fluorescence images were performed using ImageJ 1.48v (National Institutes of Health,
115 U.S.A.). Prior to analyses, the fluorescence images were confirmed as not being saturated at any pixels.
116 Three-dimensional graphs of the intensities of the pixels were generated using Surface Plot command.
117 The fluorescence intensity of individual bacteria was measured using Particle Analysis command. A
118 background value (bacteria-absent area) was used as a threshold for particle detection. A range of
119 particle area was set to detect only individual and not-overlapping bacterial cell images.

120

121 *Growth curve*

122 Growth curves were determined as previously described with some modifications (Minaba and Kato,
123 2014). Overnight cultures of bacteria were diluted (1:200) in fresh LB medium and were incubated at
124 37°C with rotary shaking at 200 rpm. After reaching a visible density (around $OD_{590} = 0.1$), OD_{590} was
125 measured every 20 min for 2 h.

126

127 **Results and Discussion**

128

129 To characterize the intermediate states of the translational switch using the IY-incorporation system,
130 the IY dose-dependency of translational efficiency for a target gene was first determined for a bacterial
131 population (Fig. 2A). As shown in Fig. 1, an EGFP gene containing an amber stop codon next to the
132 ATG translational start codon was constitutively transcribed by the *lpp* promoter in the *E. coli* BL21-
133 AI strain expressing IYRS and MJR1. The translational efficiency was estimated from the EGFP
134 fluorescence 6 h after IY addition into the medium. The “gross” translational efficiency for the
135 population started to increase significantly at 3×10^{-7} M and reached maximum levels at 10^{-5} M.
136 Intermediate levels of translational efficiency were observed at a 2-log_{10} suboptimal concentration of
137 IY (10^{-7} to 10^{-5} M), suggesting that the translational efficiency can be tuned in this concentration range.
138 The 50% effective concentration was estimated to be 3×10^{-6} M. The IY concentration-dependent
139 change of the gross translational efficiency was also confirmed by a direct measurement of the time
140 course for EGFP accumulation (Fig. 2B). The EGFP accumulation rate was clearly slower at
141 suboptimal concentrations than that at the optimal concentration. The accumulation rate increased with
142 increasing IY concentration, also suggesting that an intermediate translational efficiency could be
143 obtained in the suboptimal concentration range.

144 Intermediate levels of gene expression for the pooled bacteria are not always equal to that for

145 an individual bacterium. In the case of conditional gene expression by the *araBAD* promoter,
146 intermediate expression levels in the cultures reflected a population average of the induced and non-
147 induced cells, i.e., each cell responded to an inducer L-arabinose at a suboptimal concentration in an
148 all-or-none manner (Siegele and Hu, 1997; Guzman et al., 1995). A similar non-uniform induction was
149 also reported for the *lac* operon (Novick and Weiner, 1957; Maloney and Rotman, 1973). We therefore
150 determined whether the IY dose-dependent change of EGFP fluorescence in individual cells using
151 fluorescence images (Fig. 3). The fluorescence intensity of these images was quantified by image
152 analysis, and spatial maps were generated. The fluorescence intensity clearly increased with increasing
153 IY concentration. Fluorescent intensity distribution histograms of individual bacteria were also
154 examined. As expected from the fluorescence images and their spatial maps, the peak frequency at a
155 suboptimal IY concentration (1×10^{-6} M) was located between those at zero and the saturation
156 concentration, indicating that the translational efficiency of individual bacteria can be controlled at
157 intermediate values. This response is unlike the mix-population of all-or-none responding cells
158 observed in a suboptimal concentration of inducers for both the *araBAD* promoter and the *lac* operon.
159 The frequency distribution was relatively wide and overlapped with those at zero and at the saturation
160 concentration, suggesting that the responses of individual cells are variable at suboptimal
161 concentrations. The all-or-none behavior of the *lac* operon was explained by an autocatalytic positive
162 feedback loop that led to a burst of synthesis of galactoside permease LacY (Novick and Weiner, 1957;

163 Maloney and Rotman, 1973). A similar model was also proposed for the *araBAD* promoter system
164 (Siegele and Hu, 1997). In these models, the intracellular concentration of either lactose or arabinose
165 tends to be either very low or saturated. To obtain a better linear response to an extracellular inducer
166 concentration, IPTG is used instead of lactose in a *lacY⁻* strain for control of the *lac* promoter
167 (Khlebnikov and Keasling, 2002). Similarly, mutant strains in which arabinose transport and
168 degradation genes are deficient can avoid the all-or-none response of the *araBAD* promoter (Bowers et
169 al., 2004). These modifications impair the positive feedback loop and confer linearity between
170 extracellular and intracellular inducer concentrations. In the case of the IY-controlling translational
171 switch, the velocity of translation by a suppressor IY-tRNA is expected to depend on the intracellular
172 IY concentration if the concentrations of the suppressor tRNA, IYRS, and peptide release factors are
173 constant (Yarus et al., 1986). The intracellular IY concentration was possibly at a subsaturation level at
174 the suboptimal concentration of extracellular IY. Although the uptake mechanism of IY remains
175 unclear, positive feedback loops as seen in the *lac* operon or the *araBAD* system may be weak or not
176 be involved (Pittard, 1996).

177 Approximately 7% of the maximum translation was detected even in the absence of IY, as
178 also described previously (Minaba and Kato, 2014). The leaky translation was completely abolished by
179 deletion of the *MJR1* gene, suggesting that mischarges of *MJR1* were the cause (Fig. 4A and 4B).
180 Although some countermeasure techniques have been proposed, reduction of leaky translation needs to

181 be a priority (Minaba and Kato, 2014).

182 The translational efficiency decreased from the saturation level at an extremely high IY
183 concentration (Fig. 2A and 2B). Although its mechanism remains to be elucidated, the decrease may
184 not be due to non-specific toxicity of IY because the bacterial growth rates did not decrease both in the
185 IY-incorporating strains and in the parent strain (Fig. S3).

186 In this study, we evaluated the IY-controlling translational switch using a single setting (a
187 single amber codon in one position, and the single target gene EGFP). In the future, further studies
188 using this application should clarify how general this system is.

189 **Conclusions**

190

191 The translational switch using site-specific IY incorporation can be used as a “tunable translational
192 controller” that regulates the translational efficiency in each individual cell. Using this controller, we
193 expect to be able regulate the translational efficiency over a wide range in combination with any
194 transcriptional controlling systems (Minaba and Kato, 2014). The tunable translational controller is a
195 promising tool for conditional fine-tuning and for optimizing the construction of artificial gene circuits
196 in synthetic biology and in metabolic engineering (Yadav et al., 2012).

197

198

199 **Acknowledgments**

200

201 We thank Kensaku Sakamoto and Shigeyuki Yokoyama (RIKEN) for the IYRS-MJR1
202 expression plasmids and Michael Yarus (University of Colorado) for the *luxB* gene.

203

204 **REFERENCES**

205

206 **Bianco, A., Townsley, F. M., Greiss, S., Lang, K., Chin, J. W.** 2012. Expanding the genetic code of
207 *Drosophila melanogaster*. Nat. Chem. Biol. 8, 748-750.

208 **Bobrovskyy, M., Vanderpool, C. K.** 2013. Regulation of bacterial metabolism by small RNAs using
209 diverse mechanisms. Annu. Rev. Genet. 47, 209-232.

210 **Bowers, L. M., LaPoint, K., Anthony, L., Pluciennik, A., Filutowicz, M.** 2004. Bacterial expression
211 system with tightly regulated gene expression and plasmid copy number. Gene 340, 11-18.

212 **Caron, M. P., Bastet, L., Lussier, A., Simoneau-Roy, M., Massé, E, Lafontaine, D. A.** 2012. Dual-
213 acting riboswitch control of translation initiation and mRNA decay. Proc. Natl. Acad. Sci. U. S. A.
214 109, E3444-E3453.

215 **Chin, J. W., Cropp, A., Anderson, C., Mukherji, M., Zhang, Z., Schulz, P. G.** 2003. An expanded
216 eukaryotic genetic code. Science 301, 964-967.

217 **Greiss, S., Chin, J. W.** 2011. Expanding the genetic code of an animal. J. Am. Chem. Soc. 133,
218 14196-14199.

219 **Guzman, L. M., Belin, D., Carson, M. J., Beckwith, J.** 1995. Tight regulation, modulation, and high-
220 level expression by vectors containing the arabinose P_{BAD} promoter. J. Bacteriol. 177(14), 4121-
221 4130.

- 222 **Herring, C. D., Glasner, J. D., Blattner, F. R.** 2003. Gene replacement without selection: regulated
223 suppression of amber mutations in *Escherichia coli*. *Gene* 331, 153-163.
- 224 **Khlebnikov, A., Keasling, J. D.** 2002. Effect of lacY expression on homogeneity of induction from
225 the P(tac) and P(trc) promoters by natural and synthetic inducers. *Biotechnol. Prog.* 18, 672-674.
- 226 **Li, F., Zhang, H., Sun, Y., Pan, Y., Zhou, J., Wang, J.** 2013. Expanding the genetic code for
227 photoclick chemistry in *E. coli*, mammalian cells, and *A. thaliana*. *Angew. Chem. Int. Ed. Engl.* 52,
228 9700-9704.
- 229 **Liu, C. C., Schultz, P. G.** 2010. Adding new chemistries to the genetic code. *Annu. Rev. Biochem.* 79,
230 413-444.
- 231 **Maloney, P. C., Rotman, B.** 1973. Distribution of suboptimally induced β -D-Galactosidase in
232 *Escherichia coli*: the enzyme content of individual cells. *J. Mol. Biol.* 73(1), 77-91.
- 233 **Minaba, M., Kato, Y.** 2014. High-yield, zero-leakage expression system with a translational switch
234 using site-specific unnatural amino acid incorporation. *Appl. Environ. Microbiol.* 80(5), 1718-
235 1725.
- 236 **Novick, A., Weiner, M.** 1957. Enzyme induction as an all-or-none phenomenon. *Proc. Natl. Acad. Sci.*
237 U. S. A. 43(7), 553-566.
- 238 **Pittard, A. J.** 1996. Biosynthesis of the aromatic amino acids, in: Neidhardt, F. C., Durtiss III, R.,
239 Ingraham, L., Lin, C. C., Low, K. B., Magasanik, B., Reznikoff, W. S., Riley, M., Schaechter, M.,

240 Umbarger, H. E. (Eds.), *Escherichia coli* and *Salmonella*: cellular and molecular biology, 2nd ed.
241 ASM press, Washington DC, pp. 458-484.

242 **Sakamoto, K., Hayashi, A., Sakamoto, A., Kiga, D., Nakayama, H., Soma, A., Kobayashi, T.,**
243 **Kitabatake, M., Takio, K., Saito, K., Shirouzu, M., Hirao, I, Yokoyama, S.** 2002. Site-specific
244 incorporation of an unnatural amino acid into proteins in mammalian cells. *Nucleic Acids Res.* 30,
245 4692-4699.

246 **Sakamoto, K., Murayama, K., Oki, K., Iraha, F., Kato-Murayama, M., Takahashi, M., Ohtake,**
247 **K., Kobayashi, T., Kuramitsu, S., Shirouzu, M., Yokoyama, S.** 2009, Genetic encoding of 3-
248 iodo-L-tyrosine in *Escherichia coli* for single-wavelength anomalous dispersion phasing in protein
249 crystallography. *Structure* 17(3), 335-344.

250 **Schultz, D. W., Yarus, M.** 1990. A simple and sensitive *in vivo* luciferase assay for tRNA-mediated
251 nonsense suppression. *J. Bacteriol.* 172(2), 595-602.

252 **Siegele, D. A., Hu, J. C.** 1997. Gene expression from plasmids containing the *araBAD* promoter at
253 subsaturating inducer concentrations represents mixed populations. *Proc. Natl. Acad. Sci. U. S. A.*
254 94(15), 8168-8172.

255 **Yadav, V. G., Mey, M. D., Lim, C. G., Ajikumar, P. K., Stephanopoulos, G.** 2012. The future of
256 metabolic engineering and synthetic biology: towards a systematic practice. *Metab. Eng.* 14(3),
257 233-241.

- 258 **Yarus, M., Cline, S. W., Wier, P., Breeden, L., Thompson, R. C.** 1986. Actions of the anticodon
259 arm in translation on the phenotypes of RNA Mutants. *J. Mol. Biol.* 192, 235-255.
- 260 **Zengel, J. M., Lindahl, L.** 1981. High-efficiency, temperature-sensitive suppression of amber
261 mutations in *Escherichia coli*. *J. Bacteriol.* 145, 459-465.

264 **FIGURE LEGENDS**

265

266 **Fig. 1.** Schematic of the translational switch using the amber codon-specific IY. An amber stop codon
267 is inserted next to the ATG translational start codon in the target gene (*egfp*). MJR1 is an amber
268 suppressor tRNA. IYRS is an aminoacyl-tRNA synthetase that orthogonally recognizes IY and MJR1.
269 Extracellular IY is taken up by the bacteria. The addition of IY in the media results in amber stop
270 codon read-through and translation of the target gene. Translation is interrupted in the absence of IY.
271 RF1, peptide chain release factor 1.

272

273 **Fig. 2.** IY dose-dependent change in translational efficiency for a bacterial population. The
274 experimental system is schematically shown in Fig 1. (A) Dose-response curve. Bacteria were cultured
275 in media containing various concentrations of IY for 6 h. Colored circles indicate the samples for Fig. 3.
276 Data are shown as mean \pm SEM. n = 3 independent experiments. Statistical analysis was performed
277 using Welch's *t*-test in Excel ver. 14.0.7140.5002. (B) Time course of EGFP accumulation.

278

279 **Fig. 3.** EGFP expression in individual bacteria. The sampling points are indicated in the dose-response
280 curve in Fig 2A. Upper and lower photographs are epifluorescence images and Nomarski differential
281 interference contrast images, respectively. The photographic conditions were constant for all of the

282 fluorescence images. Calibration bar = 100 μm . Asterisks in spatial distribution graphs indicate the
283 upper right corners of the fluorescence images. The frequency in the histograms indicates the number
284 of individual bacteria.

285

286 **Fig. 4.** Leaky translation in the absence of IY. (A) Leaky translation for a bacterial population. Note
287 that the measured fluorescence contains both EGFP-fluorescence and non-EGFP background.
288 Complete set, the strain carrying the plasmid pTYR MjIYRS2-1(D286) MJR1 \times 3 and the amber-
289 inserted EGFP expression plasmid (driven by the *E. coli lpp* promoter); Δ MJR1, a derivative strain
290 carrying a MJR1-deleted plasmid; Δ EGFP, a derivative strain lacking the amber-inserted EGFP gene
291 expression plasmid; Δ EGFP+Lux, a derivative strain in which the amber-inserted EGFP gene was
292 substituted with an amber-inserted *LuxB* gene from the bacterium *Vibrio harveyi* as a vector control
293 (Shultz and Yarus, 1990). Data are shown as mean \pm SEM. n = 3 independent experiments. Statistical
294 analysis was performed using Welch's *t*-test. ns, not significant. (B) Observation of leaky translation in
295 individual bacteria. The EGFP fluorescence was measured in the absence of IY. In these images, non-
296 specific background fluorescence was completely filtered out (note that this method is distinct from
297 that of Fig. 4A). The exposure time for the EGFP images was twice that in Fig. 3.

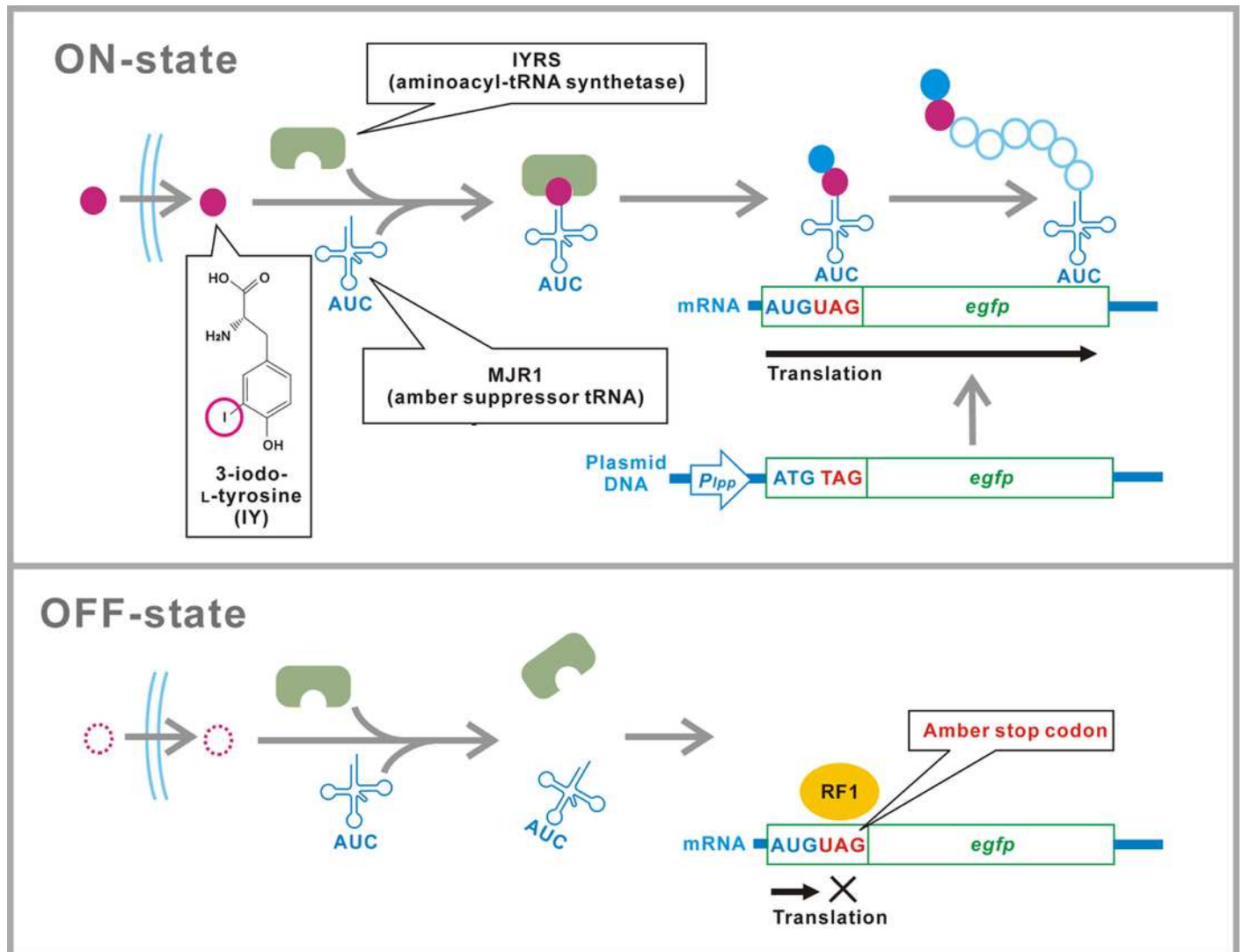
298

299

1

Schematic of the translational switch using the amber codon-specific IY.

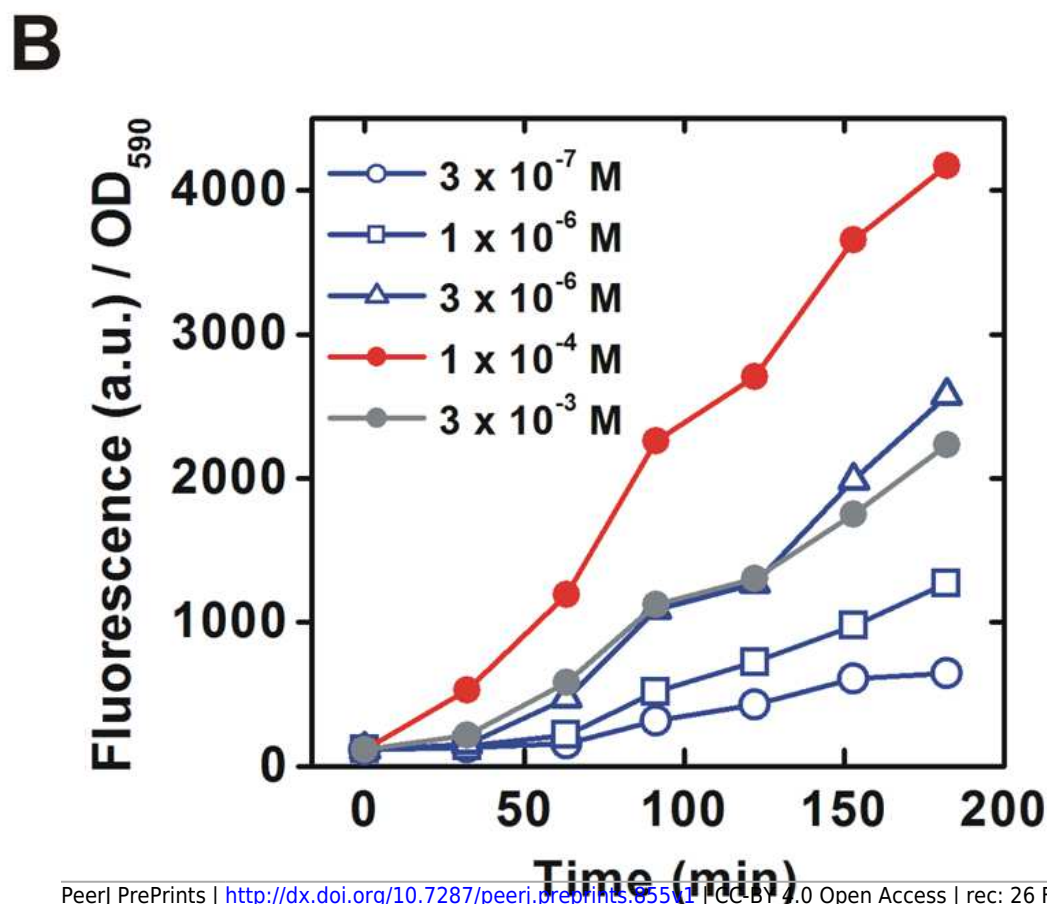
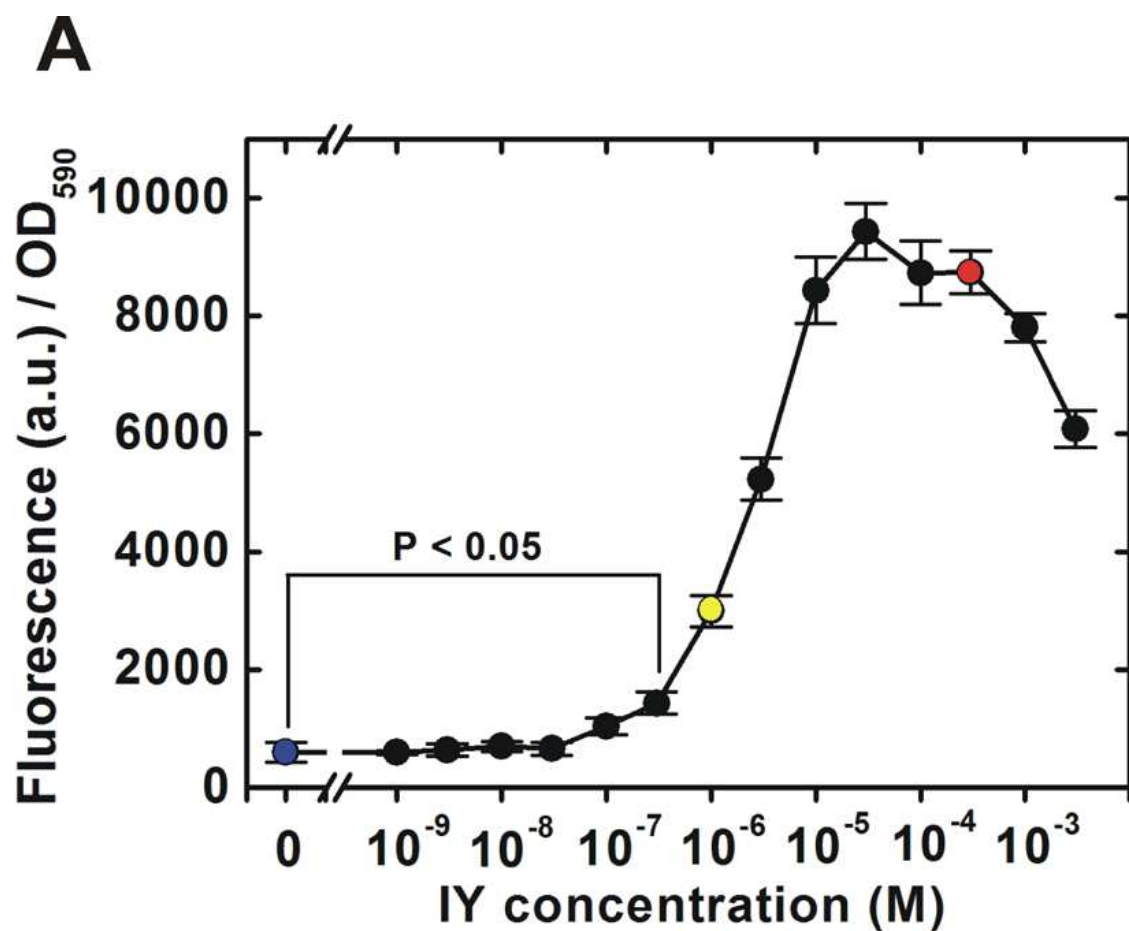
An amber stop codon is inserted next to the ATG translational start codon in the target gene (*egfp*). MJR1 is an amber suppressor tRNA. IYRS is an aminoacyl-tRNA synthetase that orthogonally recognizes IY and MJR1. Extracellular IY is taken up by the bacteria. The addition of IY in the media results in amber stop codon read-through and translation of the target gene. Translation is interrupted in the absence of IY. RF1, peptide chain release factor 1.



2

IY dose-dependent change in translational efficiency for a bacterial population.

The experimental system is schematically shown in Fig 1. (A) Dose-response curve. Bacteria were cultured in media containing various concentrations of IY for 6 h. Colored circles indicate the samples for Fig. 3. Data are shown as mean \pm SEM. n = 3 independent experiments. Statistical analysis was performed using Welch's t-test in Excel ver. 14.0.7140.5002. (B) Time course of EGFP accumulation.



3

EGFP expression in individual bacteria.

The sampling points are indicated in the dose-response curve in Fig 2A. Upper and lower photographs are epifluorescence images and Nomarski differential interference contrast images, respectively. The photographic conditions were constant for all of the fluorescence images. Calibration bar = 100 μm . Asterisks in spatial distribution graphs indicate the upper right corners of the fluorescence images. The frequency in the histograms indicates the number of individual bacteria.

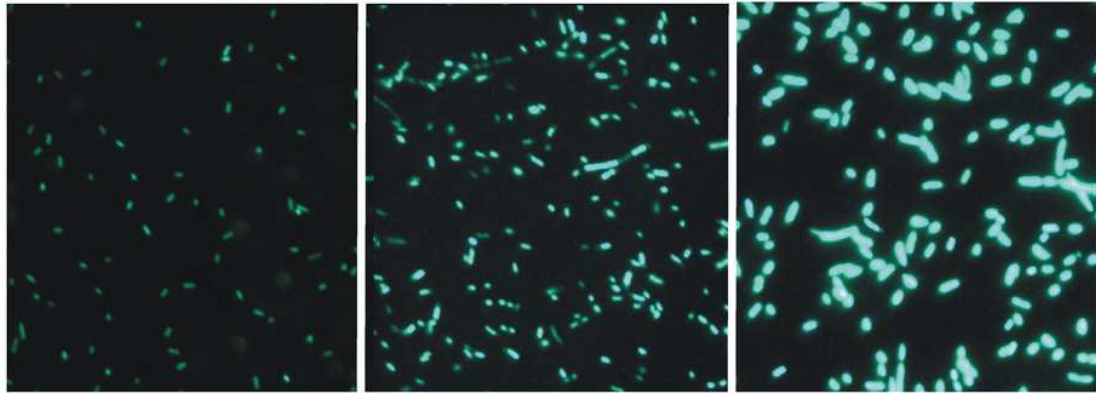
IY concentration (M)

0
(●)

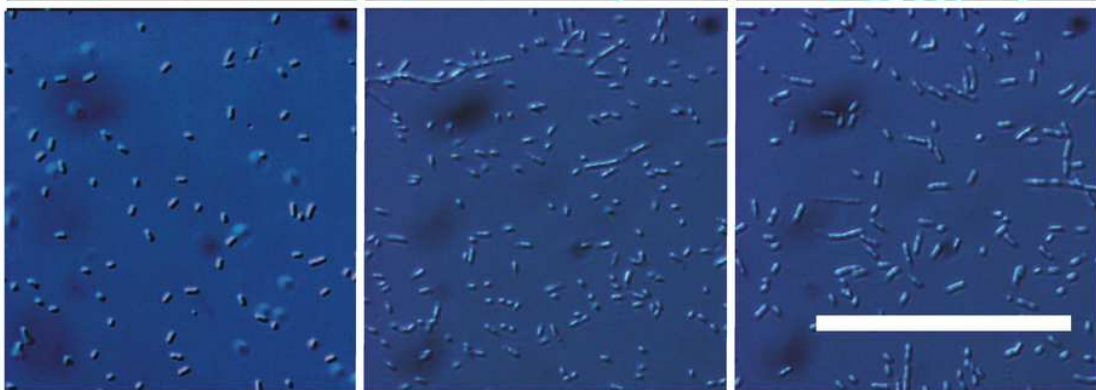
1×10^{-6}
(●)

3×10^{-4}
(●)

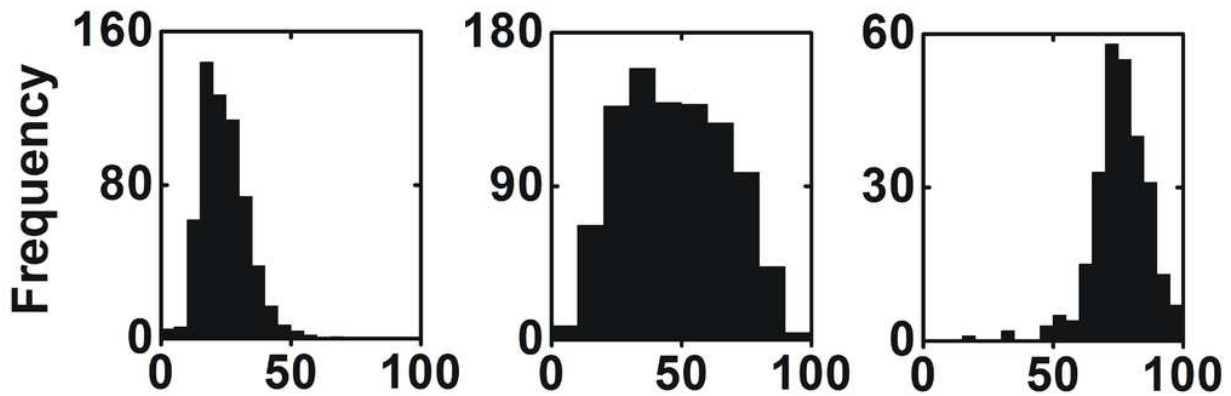
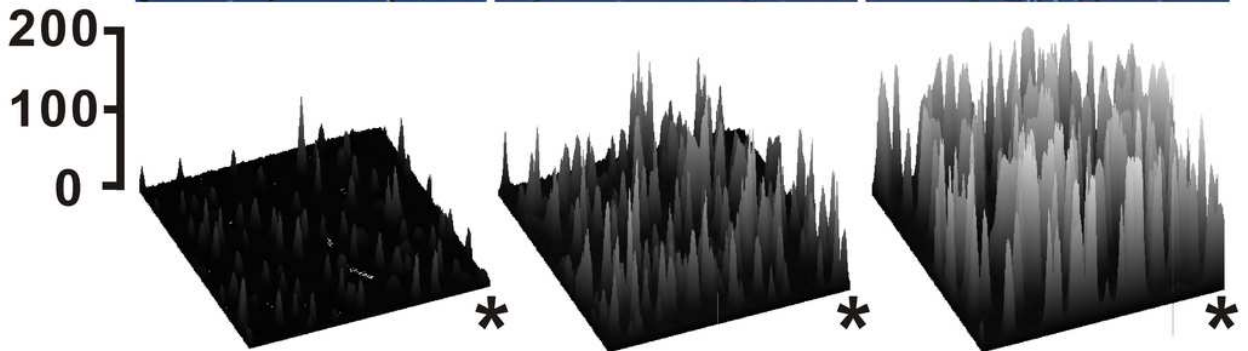
GFP



DIC



Fluorescence (a.u.)



4

Leaky translation in the absence of IY.

(A) Leaky translation for a bacterial population. Note that the measured fluorescence contains both EGFP-fluorescence and non-EGFP background. Complete set, the strain carrying the plasmid pTYR MjIYRS2-1(D286) MJR1 \square 3 and the amber-inserted EGFP expression plasmid (driven by the E. coli lpp promoter); Δ MJR1, a derivative strain carrying a MJR1-deleted plasmid; Δ EGFP, a derivative strain lacking the amber-inserted EGFP gene expression plasmid; Δ EGFP+Lux, a derivative strain in which the amber-inserted EGFP gene was substituted with an amber-inserted LuxB gene from the bacterium *Vibrio harveyi* as a vector control (Shultz and Yarus, 1990). Data are shown as mean \square SEM. n = 3 independent experiments. Statistical analysis was performed using Welch's t-test. ns, not significant. (B) Observation of leaky translation in individual bacteria. The EGFP fluorescence was measured in the absence of IY. In these images, non-specific background fluorescence was completely filtered out (note that this method is distinct from that of Fig. 4A). The exposure time for the EGFP images was twice that in Fig. 3.

